IEEE Access
Multidisciplinary | Rapid Review | Open Access Journal

Received June 7, 2018, accepted July 26, 2018, date of publication August 21, 2018, date of current version October 12, 2018.

Digital Object Identifier 10.1109/ACCESS.2018.2866387

Reliability Evaluation of Tidal Current Farm Integrated Generation Systems Considering Wake Effects

ZHOUYANG REN[1], (Member, IEEE), HUI LI[1], WENYUAN LI[1], (Life Fellow, IEEE), XUEQIAN ZHAO[2], YIHAO SUN[3], TE LI[4], AND FAN JIANG[5]

[1]State Key Laboratory of Power Transmission Equipment & System Security and New Technology, Chongqing University, Chongqing 400044, China
[2]State Grid Beijing Electric Power Research Institute, Beijing 1310905, China
[3]State Grid Henan Economic Research Institute, Zhengzhou 450052, China
[4]State Grid Zhejiang Electric Power Research Institute, Hangzhou 310008, China
[5]State Grid Chongqing Electric Power Company Maintenance Branch Company, Chongqing 400039, China

Corresponding author: Zhouyang Ren (rzhouyang1108@163.com)

This work was partially supported by the National Natural Science Foundation of China (Project No. 51607014), the Science Innovation Programs Led by Academicians in Chongqing (Project No. cstc2018jcyj-yszxX0001), the National "111" Project of China (Project No. B08036), and the Visiting Scholar Project of State Key Laboratory of Power Transmission Equipment & System Security and New Technology at Chongqing University (Project No. 2007DA10512714402).

ABSTRACT Based on a sequential Monte–Carlo simulation technique, a reliability evaluation method and several indices are proposed for tidal current farm integrated generation systems in this paper. A tidal current velocity model is first developed to capture the chronology and randomness of tidal current velocity by combining a fuzzy equivalent matrix-based clustering approach with a nonparametric probabilistic modeling technique. The single and multiple wake effects between tidal current turbines in a tidal current farm are quantitatively represented using an analytical wake model. Second, a power output model for a tidal current farm (TCF) is proposed, incorporating the characteristics of tidal current velocity, wake effects and turbine failures. A sequential Monte–Carlo simulation-based reliability evaluation method, as well as several reliability evaluation indices are proposed to quantify the impacts of TCF integration and wake effects on the reliability level of generation systems. The historical tidal current velocity data collected from a site located in FL, USA, and the popular reliability test system known as RBTS with an additional TCF were used to verify the accuracy and effectiveness of the proposed method. The impacts of tidal power integration and the relative distances between turbines in TCF on generation systems' reliability were also studied.

INDEX TERMS Tidal current generation, wake effects, reliability evaluation, sequential Monte Carlo, power system planning.

I. INTRODUCTION

Renewable energy has been intensively investigated and developed to address the challenges of climate change and growing energy demands worldwide in recent years. Tidal current generation (TCG), which generates electricity by extracting kinetic energy from tidal flows, has attracted ever-increasing attention because of its huge energy potential and renewability [1]. TCG projects have been emerging in large numbers in many countries, such as China and the UK. It is foreseeable that TCG will play a more prominent role in future power systems [2], [3].

The reliability level and planning strategies of generation systems will be unavoidably changed by the integration of TCG. It is necessary to investigate reliability evaluation methods and indices to analyze the impacts of TCG integration to help achieve a better tradeoff between the reliability and the economic efficiency of generation systems.

TCG is characterized by the following features [4]:

1) Chronology, bi-direction and randomness of tidal power. Tide mainly results from the interaction of gravitational forces between the sun, the moon, and the Earth [3], [5]. Consequently, the chronology and regularity of tidal current velocity (TCV) are revealed, i.e., TCV variation follows several specific patterns and the TCVs at adjacent time points are strongly correlated with each other. Moreover, the tidal current always flows in two opposite directions because of the nature of tide. TCV is also affected by several random factors, such as wind and wave interaction, surges and turbulence. Hence, TCV displays complex characteristics involving strong chronology and weak randomness [6]. Correspondingly, the power outputs of tidal current turbines (TCTs) show similar characteristics since there is a cubic relationship between TCT output and TCV.

2) The wake effects between TCTs in a tidal current farm (TCF). A TCT extracting kinetic energy from tidal flow causes velocity reduction in the downstream tidal flow. This phenomenon is called a wake effect. Obviously, the outputs of TCTs located downstream and the total TCF output are decreased by wake effects [7].

The previously mentioned TCG characteristics are crucial to model the behavior of TCF output and should be accurately captured in the reliability evaluation of generation systems. To the best of our knowledge, little work has been done on the reliability analysis of TCG integrated generation systems. A reliability evaluation method was proposed in [8] for the tidal power generation system (TPGS) with a doubly fed induction generator (DFIG). The failure rates of major components in a TPGS including the rotor side converter, the grid side converter, and three different operation modes of DFIG were all taken into account in evaluating the reliability of a TPGS. However, the impact of TCG integration on the reliability of generation systems has not been addressed. A reliability evaluation method for a hybrid generation system including TCG, wind power and battery energy storage was proposed in [9]. Based on the historical data of TCV and the Wakeby distribution, hourly probabilistic models for four different seasons were independently developed; i.e., 96 Wakeby distribution models were used to capture the randomness of TCV at each hour in each season. Unfortunately, the chronology of TCV and wake effects were missed with this method. Furthermore, there is no effective index for evaluating the impact of TCG integration on the reliability level of generation systems.

Other tidal power-related work has mainly focused on the optimal layout of TCT arrays [10], [11], planning and operation analyses [12]–[15]. Although much work has been done on the probabilistic modeling of PV and wind power, and reliability evaluation of generation systems incorporating PV or wind power [16]–[18], these methods cannot be directly used for tidal power integrated generation systems since both PV and wind power display stronger randomness and much weaker or little chronology compared with tidal power.

It can be deduced from the above review of literature that the characteristics of tidal power have not been fully considered in the reliability evaluation of generation systems by the existing methods, which may lead to inaccurate reliability evaluation results or inappropriate planning strategies. In this paper, a sequential Monte Carlo-based reliability evaluation method is proposed for generation systems incorporating TCF. The main contributions of this paper are listed as follows.

1) A time series model for TCF power output is proposed. The chronology, randomness and bi-direction of TCV are all considered, as well as the multiple wake effects of tidal flow and TCTs failures.
2) A sequential reliability evaluation method and eight reliability evaluation indices are proposed to quantify the impacts of TCG integration and wake effects on the reliability level of generation systems. The historical data of TCV and RBTS were used to test the effectiveness and accuracy of the proposed method.

The rest of this paper is organized as follows. The TCF power output time series model is developed in Section II. The reliability evaluation method for a generation system incorporating TCF is proposed in Section III. Case studies are provided in Section IV, followed by conclusions in Section V.

II. THE TCF POWER OUTPUT TIME SERIES MODEL

The simulation of tidal power time series is an important part of the sequential reliability analysis of generation systems incorporating TCF. In this section, a model of TCF power output time series is presented to capture the characteristics of TCV, turbine wake effects and TCT failures. The framework of the proposed model is shown in Fig. 1. First, a fuzzy equivalent matrix-based clustering approach is combined with a nonparametric kernel density estimation method to capture the strong chronology and weak randomness of TCV. Second, an analytical model is introduced to simulate turbine wake effects and estimate the TCV reduction for each TCT in a TCF while considering the bi-direction of TCV. Next, the TCT power output is further modeled by taking stochastic turbine failures into account. Finally, the TCF power output time series model is developed by combining the models of TCV, wake effects and TCT power output.

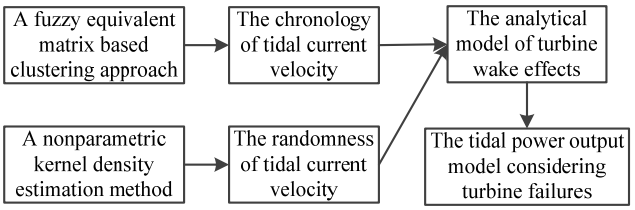

FIGURE 1. The TCF power output time series model.

A. THE MODEL OF TIDAL CURRENT VELOCITY

The chronology and regularity of TCV can be efficiently simulated by using a clustering technique. The k-means clustering technique [19] is popular and widely used in power system analysis. Unfortunately, it is sensitive to the initial cluster centers, which means the result of classification may be undesirable. A fuzzy equivalent matrix-based approach (FEMBA) is adopted in this section, which does not require any initial cluster center setting. Furthermore, in FEMBA, the membership functions can be derived from the historical TCV data without requiring any user's subjective experience [20].

Assume that there are n historical day curves of TCV at a specific location, which can be represented as $\mathbf{V} = \{\mathbf{V}_1, \mathbf{V}_2, \ldots, \mathbf{V}_n\}$, in which $\mathbf{Vi} = [v_{i1}, v_{i2}, \ldots, v_{id}]$ denotes the ith day curve of TCV, where $i = 1, 2, \ldots, n$, and d is the number of time points in one day. The set of n historical day curves $\mathbf{V}$ can be expressed in matrix form and is shown as follows, where each row denotes a day curve of TCV.

$$\mathbf{V} = \begin{bmatrix} v_{11} & v_{12} & \cdots & v_{1d} \\ v_{21} & v_{22} & \cdots & v_{2d} \\ \vdots & \vdots & \vdots & \vdots \\ v_{n1} & v_{n2} & \cdots & v_{nd} \end{bmatrix} \quad (1)$$

By using FEMBA, n day curves can be categorized into several clusters, and then each cluster mean and day curves belonging to each cluster can be derived. The cluster means can be regarded as typical day curves to simulate the chronology of TCV. Classification using FEMBA includes the following steps.

1) Normalization of TCV data. The daily chronology of TCV can be captured by the shape of TCV day curve, rather than by the absolute velocity value. For instance, several TCV day curves with similar shapes may have different velocity values but follow the same pattern. Hence, all the TCV day curves should be normalized using their peak values; the corresponding formula is shown in (2). After normalization, all the TCV data are in the interval [0, 1].

$$v'_{ij} = \frac{v_{ij}}{\max\{v_{i1}, v_{i2}, \ldots, v_{id}\}} \tag{2}$$

where v_{i1}, v_{i2}, v_{id} is the TCV at the first, second and dth time point on the ith historical day curve of TCV, respectively. The v'_{ij} is the normalized value of v_{ij}.

2) Similarity quantification. The correlation coefficient is adopted to quantify the degree of nearness between TCV day curves, which can be calculated by

$$r_{ih} = \frac{\sum_{j=1}^{d} \left| v'_{ij} - \overline{v_i} \right| \left| v'_{hj} - \overline{v_h} \right|}{\sqrt{\sum_{j=1}^{d} \left(v'_{ij} - \overline{v_i} \right)^2} \sqrt{\sum_{j=1}^{d} \left(v'_{hj} - \overline{v_h} \right)^2}} \tag{3}$$

where, r_{ih} denotes the correlation coefficient of the ith and hth day curves of TCV, v'_{hj} is the TCV at the jth time point on the hth day curve after normalization. $\overline{v_i}$ and $\overline{v_h}$ are the average value of the ith and hth normalized day curves, respectively and can be calculated by

$$\overline{v_i} = \frac{1}{d} \sum_{j=1}^{d} v'_{ij} \quad \overline{v_h} = \frac{1}{d} \sum_{j=1}^{d} v'_{hj} \tag{4}$$

It can be observed from (3) that the value of r_{ij} is in the interval [0, 1]. The closer r_{ij} is to 1, the more similarity the two TCV day curves have. Using (3) and (4), the correlation coefficients between all the day curves can be derived, and the following n-order fuzzy relation matrix $\mathbf{R}$ can be formulated.

$$\mathbf{R} = \begin{bmatrix} r_{11} & r_{12} & \cdots & r_{1n} \\ r_{21} & r_{22} & \cdots & r_{2n} \\ \vdots & \vdots & \vdots & \vdots \\ r_{n1} & r_{n2} & \cdots & r_{nn} \end{bmatrix} \tag{5}$$

$\mathbf{R}$ shows the following two features:

a) $\mathbf{R}$ is a symmetric matrix since $r_{ij} = r_{ji}$.
b) $\mathbf{R}$ is a fuzzy reflexivity matrix since $r_{ii} = 1$.

Hence, $\mathbf{R}$ is a fuzzy similarity relation matrix and each element in $\mathbf{R}$ represents the degree of similarity between two TCV day curves. It should also be noted that the correlation coefficients in $\mathbf{R}$ cannot be directly used to cluster TCV day curves, since $\mathbf{R}$ does not have the feature of transferability. In other words, if A is similar to B, and B is similar to C, it cannot be guaranteed that A is similar to C.

3) The square method (SM) is used to transform $\mathbf{R}$ into a fuzzy equivalence matrix with the feature of transferability. The main steps of the SM are as follows.

a) $\mathbf{R}^2$ can be acquired through self-multiplication, which is defined as

$$\mathbf{R}^2 = \mathbf{R} \circ \mathbf{R} \tag{6}$$

where, the symbol denotes the operation of self-multiplication. The element r_{ij}^2 of $\mathbf{R}^2$ can be calculated by

$$r_{ij}^2 = \max\left\{\min\left\{r_{ik}, r_{kj}\right\} | i,\ j,\ k = 1, 2, \ldots, n\right\} \tag{7}$$

b) Perform the following self-multiplication until $\mathbf{R}^{2h} = \mathbf{R}^{2(h-1)}$ or $l \geq (\log_2 n + 1)$. And then, let $\mathbf{R}' = \mathbf{R}^{2h}$, where, $\mathbf{R}'$ denotes the desired fuzzy equivalence matrix with the feature of transferability.

$$\mathbf{R}^2 \to \left(\mathbf{R}^2\right)^2 \to \left(\mathbf{R}^2\right)^3 \to \cdots \to \mathbf{R}^{2h} = \mathbf{R}' \tag{8}$$

The elements in $\mathbf{R}'$ can be regarded as transferable similarity coefficients and can be used to classify the day curves of TCV by choosing a threshold.

4) Select a number in the interval [0, 1] as a clustering threshold. Check the diagonal elements and coefficients in the lower triangle block of $\mathbf{R}'$ column by column; if the coefficients are equal to or larger than the selected threshold, then the corresponding TCV day curves are classified into one cluster. If a day curve cannot be classified by this procedure, it is in a cluster by itself.

After classification, the mean of each cluster and the day curves belonging to each cluster can be obtained. The direction information of tidal current for each cluster mean is retained by averaging the angle of tidal current at each time point on day curves belonging to the same cluster.

By taking the cluster mean value away from TCV day samples belonging to the same cluster, the samples of the stochastic component of TCV at each time point can be derived to simulate the randomness of TCV. For example, for the eth cluster, the mean is denoted as $\mathbf{M_e} = [m_{e1}, m_{e2}, \ldots, m_{ed}]$, and $\mathbf{V_{ei}} = [v_{ei1}, v_{ei2}, \ldots, v_{eid}]$ is the ith day curve of TCV belonging to the eth cluster. The corresponding stochastic component S_{eij} of v_{eij} can be derived by

$$S_{eij} = v_{eij} - m_{ej} \tag{9}$$

Next, the probability distribution for the stochastic component of TCV at each time point can be estimated using a nonparametric kernel density estimation technique.

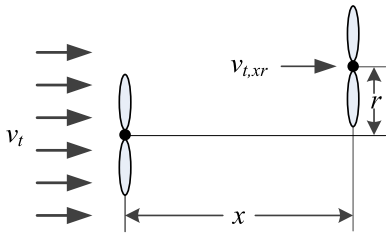

FIGURE 2. Turbine wake effect.

For example, the probability density function f of the stochastic component is estimated by [21] and [22]

$$f\left(S_j\right) = \frac{1}{nh}\sum_{e=1}^{k}\sum_{i=1}^{n_e} G\left(\frac{S_j - S_{eij}}{h}\right) \tag{10}$$

where, S_j is the stochastic component at the jth time point, $f(S_j)$ is the probability density function of S_j, G is the kernel function and is often chosen as a Gaussian distribution function, h is the bandwidth, k is the number of clusters, n_e is the number of day curves belonging to the eth cluster, and n is the total number of TCV day curves. Obviously, $n = k^* n_e$.

B. THE ANALYTICAL MODEL OF TURBINE WAKE EFFECTS

The generation behavior of a TCT is affected by other TCTs located upstream, which should be considered in the estimation of TCF output. An analytical wake model [23] is introduced to model the turbine wake property and quantify the TCV reduction caused by the turbine wake effects for each TCT.

A turbine wake effect between two TCTs is shown in Fig. 2. The TCV reduction downstream of a TCT can be estimated by [23]

$$v_{t,xr} = v_t - (v_t - v_{t,min})e^{[-((r+0.081x-(D/2))^2/(2(0.081x)^2))]} \tag{11}$$

where v_t is the incoming TCV at the tth time point. $v_{t,xr}$ is the velocity of tidal current flowing to the downstream TCT with the lateral distance x and the vertical distance r. D is the diameter of the TCT disc. $v_{t,min}$ is the minimum velocity along the downstream of a TCT wake and can be calculated by [23]

$$v_{t,min} = v_t\sqrt{1 - C_T}\,(0.0927\,(x/D) + 0.993) \tag{12}$$

where C_T is the thrust coefficient of the TCT.

The mutual interaction of turbine wakes exists in a TCF and the incoming flow of a TCT may be influenced by more than one TCT upstream in the same TCF. Undoubtedly, multiple wake effects must be simulated to evaluate the TCF output. The inflow velocity of the ith TCT under multiple wake effects of upstream TCTs can be calculated by [23]

$$v_{t,i} = v_{t,o} - \sqrt{\sum_{j=1,j\neq i}^{N_t}\left(v_{t,j} - v_{t,ij}\right)^2} \tag{13}$$

where $v_{t,i}$ is the TCV of the ith TCT under multiple wake effects at the tth time point. $v_{t,o}$ is the incoming velocity of the ith TCT at the tth time point without a wake effect. N_t is the number of TCTs affecting the TCV of the ith TCT. $v_{t,j}$ is the TCV of the jth TCT at the tth time point. $v_{t,ij}$ is the TCV of the ith TCT at the tth time point considering only the wake effect of the jth TCT.

It should be noted that the TCV distribution in a TCF is influenced by the direction of incoming tidal current. Since the incoming tidal current of TCF can be considered as bidirectional flow, the TCF is usually located at the main direction of tidal current. Consequently, Eqs. (11)-(13) can be directly used to quantify the TCV distribution in a TCF by specifying the direction of incoming tidal current.

C. MODELING TCT POWER OUTPUT WITH RANDOM FAILURES

The power output of each TCT at tth time point in a TCF can be calculated by [8]

$$P_t = \begin{cases} 0 & 0 < v_t < v_{cutin} \\ 0.5C_p\rho A v_t^3 S_{tct} & v_{cutin} \le v_t < v_{rated} \\ P_{rated}S_{tct} & v_{rated} \le v_t \end{cases} \tag{14}$$

where P_t and P_{rated} are the actual output at the tth time point and rated output of TCT, respectively. C_p is power capture coefficient and A is the area swept out by the blade of TCT. v_{cutin} and v_{rated} are the cut-in velocity and the rated TCV of TCT. v_t is the TCV at the tth time point. S_{tct} denotes the available state of the TCT at the tth time point and can be either 0 or 1. If S_{tct} equals 1, the TCT is in the up state; otherwise, the TCT is in the down state.A state duration sampling approach [19] is applied to determine the hourly state (up or down) of each TCT in a TCF. The duration D_g of a TCT residing in its present state is usually assumed to follow an exponential distribution. By using the following equation, the ith random sample of D_g can be acquired.

$$D_{gi} = \frac{1}{\lambda}\mathrm{In}R_i \tag{15}$$

where D_{gi} is the ith random sample of D_g. R_i is the ith random number uniformly distributed in the interval between 0 and 1. If the present state of a TCT is up, λ is the failure rate of the TCT; otherwise, λ is the repair rate of the TCT.

The chronological state transition processes of each TCT in a considered time span can be obtained by repeatedly sampling D_g using (15). The S_{tct} at each time point can be determined from the chronological state transition process. The chronological states of non-tidal generators in a generation system can also be determined by (15) with different random numbers.

In the paper, the TCT is assumed to incorporate the pitch control system to pitch the nacelle and the blades according to the real direction of incoming tidal current. That is to say, the power output of a single TCT is not impacted by the direction of tidal current. However, the TCV distribution in a

TCF and the total power output of a TCF are highly impacted by the direction of tidal current.

III. A RELIABILITY EVALUATION METHOD FOR GENERATION SYSTEMS INCORPORATING TCF

Sequential Monte Carlo simulation methods have been widely used in reliability evaluation of generation systems. Time-dependent variables can be incorporated, and frequency and duration indices such as loss of load frequency (*LOLF*) and loss of load duration (*LOLD*) can also be estimated [24]–[26]. In this section, a sequential Monte Carlo simulation method [19] is adopted to develop a reliability evaluation method for generation systems containing TCF. A Monte Carlo sampling method is first developed to generate stochastic samples for reliability evaluation based on the model of TCF output. Second, the reliability indices are proposed to quantify the impact of TCG integration and the wake effects on the reliability level of generation systems.

A. THE MONTE CARLO-BASED SAMPLING METHOD FOR RELIABILITY EVALUATION

The sampling procedure is as follows and the flow chart is shown in Fig. 3.

1) Input the failure and repair rates of each generator for a given generation system, n historical TCV day curves collected from a given site, the cut-in velocity, rated velocity and rated power of each TCT, and the layout information of TCTs for a given TCF. Initialize the convergence precision ε in the Monte Carlo simulation and let the iteration count $k_d = 1$.
2) Categorize the n day TCV samples using the FEMBA given in Section II-A. The means and day curves of TCV for each cluster can be acquired. The probability of each cluster can also be derived by dividing the total number of day samples by the number of samples belonging to each cluster.
3) Based on a random number following a uniform distribution between 0 and 1, randomly choose a TCV cluster. Establish a TCV model using the day curves of the selected cluster.
4) Based on the TCV model, generate stochastic samples for the stochastic components of TCV at each time point using the rejection sampling method [17]. Then, add the random samples of the stochastic components at the corresponding points to the mean curve of the selected cluster to generate a random TCV day sample.
5) Repeat Steps 3-4 until a year-long sample of TCV has been generated.
6) Randomly generate the state of each TCT in the TCF at each time point for one year using the method described in Section II-C.
7) Based on the analytical wake model given in Section II-B, produce the random TCV samples, the random state of each TCT, and the TCF output at each time point for one year.

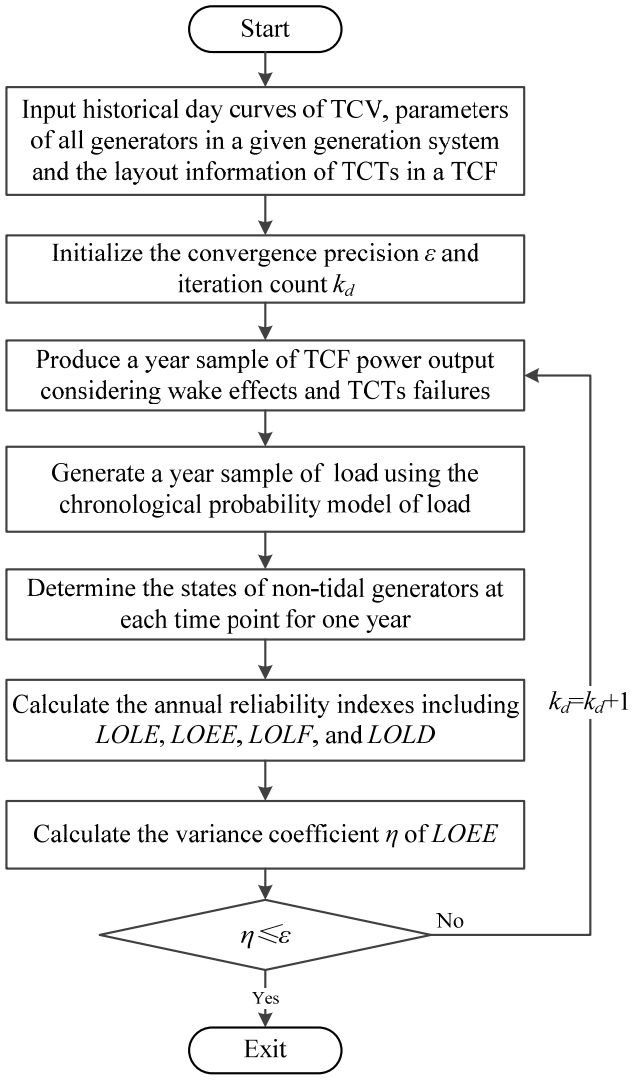

FIGURE 3. A reliability evaluation method for generation systems incorporating TCF.

8) The stochastic samples of load at each time point in one year can be generated using the chronological probability model of load given in [19].
9) Determine the states of non-tidal generators in the generation system at each time point for one year using the state duration sampling approach in Section II-C. Then, the total generation capacity of the non-tidal generators at each time point can be calculated using the capacity and state of each non-tidal generator.
10) Calculate the annual reliability indices including *LOLE* (loss of load expectation), *LOEE* (loss of energy expectation), *LOLF*, and *LOLD* using the year samples of TCF power output, other generators' power outputs and loads.
11) The variance coefficient η of *LOEE* is used as the convergence criterion in the sequential Monte Carlo simulation. If η is less than ε, exit; otherwise, let $k_d = k_d + 1$ and go back to Step 3.

B. RELIABILITY EVALUATION INDICES FOR THE TCF-INTEGRATED GENERATION SYSTEMS

Based on the *LOLE*, *LOEE*, *LOLF* and *LOLD*, the following four indices are developed to quantify the influence of TCG integration on the improvement of generation system reliability.

$$ITPLOLE = \frac{(LOLE_b - LOLE_a)}{LOLE_b} \tag{16}$$

$$ITPLOEE = \frac{(LOEE_b - LOEE_a)}{LOEE_b} \tag{17}$$

$$ITPLOLF = \frac{(LOLF_b - LOLF_a)}{LOLF_b} \tag{18}$$

$$ITPLOLD = \frac{(LOLD_b - LOLD_a)}{LOLD_b} \tag{19}$$

where *ITPLOLE*, *ITPLOEE*, *ITPLOLF* and *ITPLOLD* denote the percentage of improvement in the *LOLE*, *LOEE*, *LOLF* and *LOLD* due to the integration of tidal power, respectively. The $LOLE_b$, $LOEE_b$, $LOLF_b$ and $LOLD_b$ are the reliability indices before the integration of tidal power. The $LOLE_a$, $LOEE_a$, $LOLF_a$ and $LOLD_a$ are the reliability indices after the integration of tidal power.

Furthermore, the following four indices are presented to quantify the influence of turbine wake effects on the reliability level of generation systems.

$$CTWLOLE = \frac{(LOLE_w - LOLE_{nw})}{LOLE_{nw}} \tag{20}$$

$$CTWLOEE = \frac{(LOEE_w - LOEE_{nw})}{LOEE_{nw}} \tag{21}$$

$$CTWLOLF = \frac{(LOLF_w - LOLF_{nw})}{LOLF_{nw}} \tag{22}$$

$$CTWLOLD = \frac{(LOLD_w - LOLD_{nw})}{LOLD_{nw}} \tag{23}$$

where *CTWLOLE*, *CTWLOEE*, *CTWLOLF* and *CTWLOLD* are the percentage changes due to the turbine wake effects in the *LOLE*, *LOEE*, *LOLF* and *LOLD* indices, respectively. $LOLE_{nw}$, $LOEE_{nw}$, $LOLF_{nw}$ and $LOLD_{nw}$ are the reliability indices of the generation system without considering the turbine wake effects. $LOLE_w$, $LOEE_w$, $LOLF_w$ and $LOLD_w$ are the reliability indices of the generation system considering the turbine wake effects.

IV. CASE STUDIES

To demonstrate the accuracy and effectiveness of the proposed method and assess the impacts of TCG integration and turbine wake effects on the reliability of generation systems, cases with different TCG capacities, different TCT distances and different directions of incoming tidal current were designed and analyzed using the popular reliability test system RBTS [27] with the addition of TCF.

The RBTS is composed of 11 conventional generating units, ranging in size from 5 MW to 40 MW, with a total installed capacity of 240 MW. The hourly peak load curve consisting of 8736 load points on a per unit basis is adopted and the annual peak load is 185 MW [27].

A TCF is added to the RBTS in the case studies. The TCTs in a TCF are arranged in a rectangular layout. The parameters of the TCTs deployed in the TCF are as follows: the cut-in tidal current velocity v_{cutin} and rated tidal current velocity v_{rated} are 1.5 and 2.5 m/s, respectively; the rated power P_{rated} is 1 MW; the power capture coefficient C_p is 0.5; the thrust coefficient C_T is 0.7; the diameter of turbine D is 20 meters; and the failure and repair rates are 1.4011 failures/year and 38.1793 repairs/year, respectively [8]. The hourly measured data of the tidal current velocity used in the case studies over a period of one year are collected from a site located in Florida, USA [28].

A. CONVERGENCE ANALYSIS OF THE PROPOSED RELIABILITY METHOD FOR THE RBTS GENERATION SYSTEM CONTAINING A TCF

Assume that the RBTS is integrated with a 20 MW TCF consisting of five rows of four TCTs. The lateral and vertical distances between TCTs are 60 meters. The variance coefficient of *LOEE* is used as the convergence criterion in the proposed sequential Monte Carlo simulation method and the convergence precision ε is set to be 0.05.

The reliability indices of the RBTS incorporating a TCF reached the convergence criterion after 9897 sampling years. Table 1 shows the values of *LOLE*, *LOEE*, *LOLF* and *LOLD*. The *LOEE* and its variance coefficient versus the number of sampling years are plotted in Fig. 4. The coordinate axis on the left side of Fig. 4 denotes the variance coefficient of *LOEE*, while the coordinate axis on the right side of Fig. 4 denotes the yearly value of *LOEE*. It can be observed from Fig. 4 that both the *LOEE* and its variance coefficient

TABLE 1. Reliability indices of RBTS containing a 20 MW TCF.

LOLE (h/yr)	*LOEE* (MWh/yr)	*LOLF* (occurrences/yr)	*LOLD* (hours/occurrences)
1.0255	9.7967	0.5546	1.8491

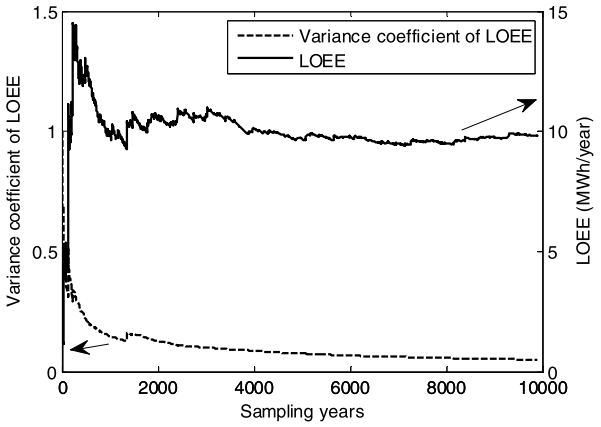

FIGURE 4. The curves of *LOEE* and its variance coefficient versus the number of sampling years.

vary sharply at the early stage. The indices gradually become stable as the number of sampling years increase.

B. RELIABILITY ANALYSIS OF THE RBTS GENERATION SYSTEM WITH DIFFERENT TCF CAPACITIES

The following four cases are designed to evaluate the impact of TCG integration on the reliability performance of the RBTS generation system.

Case 1: No TCF is connected to RBTS.

Case 2: The RBTS is integrated with a 20 MW TCF consisting of five rows of four TCTs. The lateral and vertical distances between TCTs are both set to be 60 meters.

Case 3: The RBTS is integrated with a 40 MW TCF consisting of five rows of eight TCTs. The lateral and vertical distances between TCTs are both set to be 60 meters.

Case 4: The RBTS is integrated with a 60 MW TCF consisting of six rows of ten TCTs. The lateral and vertical distances between TCTs are both set to be 60 meters.

The TCT deployment in the integrated TCF for Cases 2-4 is shown in Fig. 5, where one star denotes a TCT. The relative distances between TCTs and the position information of each TCT can be acquired from Fig. 5. For Cases 1-4, the reliability of the RBTS was evaluated using the proposed method, and the test results are shown in Table 2. It can be seen that *LOLE*, *LOEE*, *LOLF* and *LOLD* all dramatically decreased for Case 2 compared with those for Case 1, and correspondingly, *ITPLOLE*, *ITPLOEE*, *ITPLOLF* and *ITPLOLD* display significant improvement percentages due to the addition of the tidal current power integration.

The *LOLE*, *LOEE*, *LOLF* and *LOLD* indices for Cases 3 and 4 have marginal decreases compared with those for Case 2. Equivalently, the *ITPLOLE*, *ITPLOEE*, *ITPLOLF* and *ITPLOLD* indices are only marginally larger than those for Case 2. This suggests that the reliability level of RBTS is not significantly improved by the integration of more TCTs for Cases 3 and 4, although the integrated tidal current capacity is doubled or tripled compared to that in Case 2. This fact indicates that increasing more than 20 MW of tidal current generation capacity may not be an economically effective solution for further improvement of the RBTS generation system reliability. However, it should be emphasized that the conclusion is case-dependent; different conclusions may be obtained for different cases. The proposed method provides a tool in helping quantify the reliability of any generation system with TCTs.

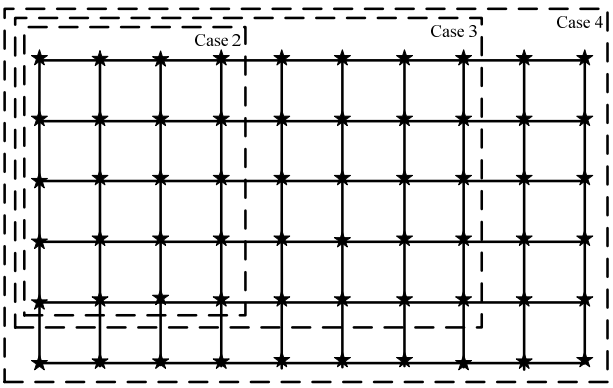

FIGURE 5. The TCT deployment in the TCF under Cases 2-4.

C. RELIABILITY ANALYSES OF THE RBTS GENERATION SYSTEM WITH DIFFERENT TCF WAKE EFFECTS

To demonstrate the impact of turbine wake effects on the reliability of the RBTS generation system, the following four cases are presented with different TCT layout scenarios.

Case A: The turbine wake effects are not considered in the reliability analysis of RBTS.

Case B: The RBTS is integrated with a 20 MW TCF consisting of five rows of four TCTs. The lateral and vertical distances between TCTs are both set to be 60 meters.

Case C: The RBTS is integrated with a 20 MW TCF consisting of five rows of four TCTs. The lateral and vertical distances between TCTs are both set to be 80 meters.

Case D: The RBTS is integrated with a 20 MW TCF consisting of five rows of four TCTs. The lateral and vertical distances between TCTs are both set to be 100 meters.

The reliability indices of the RBTS for Cases A-D were assessed using the proposed method and the test results are shown in Table 3. *LOLE* and *LOEE* increase by more than ten percent for Case B compared with Case A, whereas the *LOLF*

TABLE 2. Reliability indices for cases 1-4.

Reliability Index	Case 1	Case 2	Case 3	Case 4
LOLE (h/yr)	1.4764	1.0255	0.9829	0.9562
ITPLOLE	0	30.54%	33.43%	35.23%
LOEE (MWh/yr)	14.631	9.7967	9.2795	8.9624
ITPLOEE	0	33.04%	36.58%	38.74%
LOLF (occurrences/yr)	0.7046	0.5546	0.5605	0.5601
ITPLOLF	0	21.29%	20.45%	20.51%
LOLD (hours/occurrences)	2.0953	1.8491	1.7536	1.7072
ITPLOLD	0	11.75%	16.31%	18.52%

TABLE 3. Reliability indices for cases A-D.

Reliability index	Case A	Case B	Case C	Case D
LOLE (h/yr)	0.9256	1.0255	0.9901	0.9593
CTWLOLE	0	10.79%	6.97%	3.64%
LOEE (MWh/yr)	8.8293	9.7967	9.4951	9.1747
CTWLOEE	0	10.96%	7.01%	3.77%
LOLF (occurrences/yr)	0.5255	0.5546	0.5455	0.5350
CTWLOLF	0	5.54%	3.81%	1.81%
LOLD (hours/occurrences)	1.7614	1.8491	1.815	1.7931
CTWLOLD	0	4.98%	3.043%	1.80%

TABLE 4. Reliability indices for cases E-F.

Reliability index	Case E	Case F	ΔR
LOLE (h/yr)	1.0255	1.0757	4.90%
LOEE (MWh/yr)	9.7967	10.0959	3.05%
LOLF (occurrences/yr)	0.5546	0.58	4.58%
LOLD (hours/occurrences)	1.8491	1.8067	-2.29%

and *LOLD* increase by about five percent. This indicates that the reliability level of the RBTS with a TCF is decreased due to the turbine wake effects as the power output of the TCF is reduced by the influence of the turbine wake.

The *CTWLOLE*, *CTWLOEE*, *CTWLOLF*, *CTWLOLD* indices decline with the increase in the distance between the TCTs in a TCF, which can be seen from the results in Cases B-D. This is because the turbine wake effect becomes weaker with increasing distance between the TCTs, and the output of the TCF increases correspondingly. These results suggest that the turbine wake effects should be considered in the reliability analysis of generation systems with tidal current generators. Ignoring the turbine wake effects will lead to overly optimistic reliability indices when the distance between TCTs is small, which may result in an incorrect conclusion for planning decisions. On the other hand, the results also indicate that the turbine wake effect may be neglected if the distance between TCTs is large enough. The proposed method provides a vehicle to quantify the turbine wake effects between TCTs.

D. RELIABILITY ANALYSES OF THE RBTS GENERATION SYSTEM CONSIDERING THE DIRECTION OF INCOMING TIDAL CURRENT

In this subsection, the RBTS is integrated with a 20 MW TCF consisting of five rows of four TCTs. The lateral and vertical distances between TCTs are both set to be 60 meters. To investigate the impact of tidal current direction on the reliability level of generation systems, the following two cases are designed.

Case E: The direction of incoming tidal current of TCF is not considered in the reliability evaluation.

Case F: The direction of incoming tidal current of TCF is considered in the reliability evaluation.

Case E and Case F were analyzed using the proposed method. The derived reliability evaluation indices are shown in Table 4, where, ΔR denotes the difference of the indices under Cases E and F in percentage form. It can be seen that without considering tidal current direction, the *LOLE*, *LOEE* and *LOLF* are underestimated while the *LOLD* is overestimated. The reason is that the direction of incoming tidal current influences the TCV distribution in the TCF. Especially, when there are some TCTs in down state, the layout of TCTs in the TCF will be largely changed and the power output of TCTs and TCF are highly dependent on the velocity and direction of incoming tidal current. It can be deduced that ignoring the direction of tidal current, the power output of TCF will be overestimated and the over-optimistic reliability results will be derived.

V. CONCLUSIONS

A sequential Monte Carlo simulation-based reliability evaluation method is proposed for generation systems incorporating TCG. The TCV characteristics, turbine wake effects, and TCT failures are all modeled and incorporated by the proposed method. Eight reliability evaluation indices are developed to quantify the impacts of TCF integration and wake effects on the reliability level of generation systems. The historical TCV data collected from a site located in Florida, USA and the popular reliability test system RBTS were used to verify the accuracy and effectiveness of the proposed method. The following conclusions can be drawn:

a) The reliability level of generation systems can be largely improved by integrating tidal power sources. However, excessive integration capacity of tidal power may have only marginal effects on the further improvement in the generation system reliability level. Determining the proper integration capacity of tidal power is an important task.

b) The reliability of generation systems with tidal current generators is affected by turbine wake effects. Ignoring the turbine wake effects will lead to overly optimistic reliability analysis results when the distance between TCTs not large enough.

c) The TCV distribution in a TCF and the power output of a TCF are highly dependent on the velocity and direction of incoming tidal current. Neglecting the direction of tidal current will overestimate the power output of TCF and lead to over-optimistic reliability evaluation results.

REFERENCES

[1] T. J. Hammons, "Tidal power," *Proc. IEEE*, vol. 81, no. 3, pp. 419–433, Mar. 1993.
[2] *OES Annual Report 2014*. Accessed: Aug. 1, 2016. [Online]. Available: https://report2014.ocean-energy-systems.org/
[3] F. O. Rourke, F. Boyle, and A. Reynolds, "Tidal energy update 2009," *Appl. Energy*, vol. 87, no. 2, pp. 398–409, 2010.
[4] S. Benelghali, M. El Hachemi Benbouzid, J. F. Charpentier, T. Ahmed-Ali, and I. Munteanu, "Experimental validation of a marine current turbine simulator: Application to a permanent magnet synchronous generator-based system second-order sliding mode control," *IEEE Trans. Ind. Electron.*, vol. 58, no. 1, pp. 118–126, Jan. 2011.
[5] R. Mazumder and M. Arima, "Tidal rhythmites and their implications," *Earth-Sci. Rev.*, vol. 69, nos. 1–2, pp. 79–95, Feb. 2005.
[6] M. Liu, W. Li, C. Wang, J.Yu, and R. Billinton, "Modeling tidal current speed using a Wakeby distribution," *Electr. Power Syst. Res.*, vol. 127, no. 1, pp. 240–248, Jan. 2015.
[7] W.-H. Lam and L. Chen, "Equations used to predict the velocity distribution within a wake from a horizontal-axis tidal-current turbine," *Ocean Eng.*, vol. 79, pp. 35–42, Mar. 2014.
[8] M. Liu, W. Li, R. Billinton, J. Yu, and C. Wang, "Reliability Evaluation of a tidal power generation system considering tidal current speed," *IEEE Trans. Power Syst.*, vol. 31, no. 4, pp. 3179–3188, Jul. 2016.
[9] M. Liu, W. Li, J. Yu, Z. Ren, and R. Xu, "Reliability evaluation of tidal and wind power generation system with battery energy storage," *J. Mod. Power Syst. Clean Energy*, vol. 4, no. 4, pp. 636–647, Oct. 2016.
[10] R. Vennell, S. W. Funke, C. Stevens, T. Divett, and S. Draper, "Designing large arrays of tidal turbines: A synthesis and review," *Renew. Sustain. Energy Rev.*, vol. 41, no. 1, pp. 454–472, Jan. 2015.

[11] S. W. Funke, P. E. Farrell, and M. D. Piggott, "Tidal turbine array optimisation using the adjoint approach," *Renew. Energy*, vol. 63, no. 1, pp. 658–673, Mar. 2014.
[12] M. Kuschke, S. Pertzsch, and K. Strunz, "Modeling of tidal energy conversion systems for primary response testing," in *Proc. IEEE Power Energy Soc. Gen. Meeting*, San Diego, CA, USA, Jul. 2012, pp. 1–6.
[13] S. Obara, M. Kawai, O. Kawae, and Y. Morizane, "Operational planning of an independent microgrid containing tidal power generators, SOFCs, and photovoltaics," *Appl. Energy*, vol. 102, pp. 1343–1357, Feb. 2013.
[14] M. C. Sousounis, J. K. H. Shek, and M. A. Mueller, "Filter design for cable overvoltage and power loss minimization in a tidal energy system with onshore converters," *IEEE Trans. Sustain. Energy*, vol. 7, no. 1, pp. 400–408, Jan. 2016.
[15] M. C. Sousounis, J. K. H. Shek, and M. A. Mueller, "Modelling, control and frequency domain analysis of a tidal current conversion system with onshore converters," *IET Renew. Power Gener.*, vol. 10, no. 2, pp. 158–165, 2016.
[16] Z. Qin, W. Li, and X. Xiong, "Estimating wind speed probability distribution using kernel density method," *Electr. Power Syst. Res.*, vol. 81, no. 12, pp. 2139–2146, Dec. 2011.
[17] Z. Ren, W. Yan, X. Zhao, W. Li, and J. Yu, "Chronological probability model of photovoltaic generation," *IEEE Trans. Power Syst.*, vol. 29, no. 3, pp. 1077–1088, May 2014.
[18] Z. Qin, W. Li, and X. Xiong, "Incorporating multiple correlations among wind speeds, photovoltaic powers and bus loads in composite system reliability evaluation," *Appl. Energy*, vol. 110, no. 1, pp. 285–294, Oct. 2013.
[19] W. Li, *Risk Assessment of Power Systems: Models, Methods, and Applications*, 2nd ed. Hoboken, NJ, USA: Wiley, 2014.
[20] W. Li, J. Zhou, X. Xiong, and J. Lu, "A statistic-fuzzy technique for clustering load curves," *IEEE Trans. Power Syst.*, vol. 22, no. 2, pp. 890–891, May 2007.
[21] Z. Ren, W. Li, R. Billinton, and W. Yan, "Probabilistic power flow analysis based on the stochastic response surface method," *IEEE Trans. Power Syst.*, vol. 31, no. 3, pp. 2307–2315, May 2016.
[22] W. K. Härdle, M. Müller, S. Sperlich, and A. Werwatz, *Nonparametric and Semiparametric Models*. Berlin, Germany: Springer, 2004.
[23] W.-H. Lam, L. Chen, and R. Hashim, "Analytical wake model of tidal current turbine," *Energy*, vol. 79, pp. 512–521, Jan. 2015.
[24] C. T. Kiranoudis and Z. B. Maroulis, "Effective short-cut modelling of wind park efficiency," *Renew. Energy*, vol. 11, no. 4, pp. 439–457, Aug. 1997.
[25] R. Billinton, H. Chen, and R. Ghajar, "A sequential simulation technique for adequacy evaluation of generating systems including wind energy," *IEEE Trans. Energy Convers.*, vol. 11, no. 4, pp. 728–734, Dec. 1996.
[26] G. Li *et al.*, "Risk analysis for distribution systems in the northeast U.S. under wind storms," *IEEE Trans. Power Syst.*, vol. 29, no. 2, pp. 889–898, Mar. 2014.
[27] R. Billinton *et al.*, "A reliability test system for educational purposes-basic data," *IEEE Trans. Power Syst.*, vol. 4, no. 3, pp. 1238–1244, Aug. 1989.
[28] *Tidal Current Data*. Accessed: May 1 2016. [Online]. Available: http://tidesandcurrents.noaa.gov/gmap3/index.shtml?type=CurrentData&region=

ZHOUYANG REN (M'14) received the Ph.D. degree in electrical engineering from Chongqing University, Chongqing, China, in 2014. He is currently an Associate Professor with the School of Electrical Engineering, Chongqing University, where he is also a Researcher with the Power and Energy Reliability Research Center. His research interests include power system reliability assessment and power system data analysis.

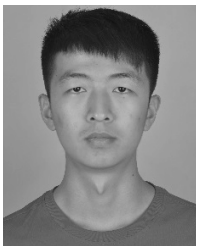

HUI LI is currently pursuing the M.S. degree with the School of Electrical Engineering, Chongqing University, Chongqing, China. His research interests include planning and operation analyses of tidal current generation integrated power system, and the reliability assessment of tidal current farm.

WENYUAN LI (SM'89–F'02–LF'17) is currently a Professor with Chongqing University, China. His research interests include power system planning, operation, optimization, and reliability assessment. He is a fellow of the Canadian Academy of Engineering and the Engineering Institute of Canada, and a Foreign Member of the Chinese Academy of Engineering. He has received several IEEE PES awards, including the IEEE PES Roy Billinton Power System Reliability Award in 2011 and the IEEE Canada Electric Power Medal in 2014.

XUEQIAN ZHAO received the M.S. degree in electrical engineering from Chongqing University, Chongqing, China, in 2012. He is currently a Specialist with the State Grid Beijing Electric Power Research Institute, Beijing, China. His research interests include asset management and power system reliability evaluation.

YIHAO SUN is currently a Senior Engineer with the State Grid Henan Economic Research Institute, Zhengzhou, China. His research interests include reliability evaluation and planning of distribution power grids.

TE LI received the M.S. degree in electrical engineering from Chongqing University, Chongqing, China, in 2012. He is currently an Engineer with the State Grid Zhejiang Electric Power Research Institute, Hangzhou, China. His research interests include lightning protection, insulation selection of transmission line, and power system reliability evaluation.

FAN JIANG is currently an Engineer with the State Grid Chongqing Electric Power Company Maintenance Branch Company, Chongqing, China. His research interests include power system reliability evaluation and asset management.